

## Novel metric describing anoxia in lakes

1 Original article

2 Anoxic age as a new tool to predict biogeochemical  
3 consequences of oxygen depletion in lakes

4

5 Running head: Novel metric describing anoxia in lakes

6

7 Richard LaBrie<sup>1</sup>, Michael Hupfer<sup>2</sup> and Maximilian P. Lau<sup>1,2, #</sup>

8 <sup>1</sup> Interdisciplinary Environmental Research Centre, TU Bergakademie Freiberg, Akademiestraße

9 6, 09599 Freiberg, Germany

10 <sup>2</sup> Leibniz Institute of Freshwater Ecology and Inland Fisheries (IGB), Müggelseedamm 310,

11 12587 Berlin, Germany

12 # Corresponding author: [maximilian.lau@ioez.tu-freiberg.de](mailto:maximilian.lau@ioez.tu-freiberg.de)

13 Author contribution statement: RL, MH and MPL did the field work, MPL developed the

14 manuscript idea, RL analyzed the data and MPL contributed, RL wrote and MPL contributed to

15 writing the first draft

16 ORCID

17 RL: 0000-0003-1681-4888

18 MH: 0000-0002-8878-1045

19 MPL: 0000-0002-0675-663X

20

21

22

23

24

## Novel metric describing anoxia in lakes

### 25 Abstract

26 Lake deoxygenation is of growing concern because it threatens ecosystem services delivery.  
27 Complete deoxygenation, anoxia, is projected to prolong and expand in lakes, promoting the  
28 production or release of nutrients, greenhouse gases and metals from water column and the  
29 sediments. Accumulation of these compounds cannot be easily predicted thus hindering our  
30 capacity to forecast the ecological consequences of global changes on aquatic ecosystems. Here,  
31 we used lakes Arendsee and Mendota monitoring data to develop a novel metric, anoxic age,  
32 characterizing lake hypolimnetic anoxia. Anoxic age explained, as a single predictor, 44% to  
33 58% of the variation for ammonium, soluble reactive phosphorus and a dissolved organic matter  
34 fluorophore. Anoxic age could be modelled using only two oxygen profiles and lake bathymetry,  
35 making it an easily applicable tool to interpret and extrapolate biogeochemical data. This novel  
36 metric thus has the potential to transform widely available oxygen profiles into an ecologically  
37 meaningful variable.

### 38 Scientific Significance Statement

39 Oxygen depletion in deep water layers of lakes is of growing concern as it expands due to  
40 eutrophication and climate change. Anoxia is deleterious to benthic invertebrates and fishes,  
41 enables the production of potent greenhouse gases and releases stored phosphorus from  
42 sediments, among others. However, quantitatively forecasting the consequences of anoxia  
43 remains a challenge. Here, we developed a novel metric, anoxic age, which may be derived from  
44 oxygen profiles to predict end-of-summer concentration of various water chemical parameters.  
45 We argue that all by-products of anaerobic microbial metabolism should be related to anoxic age

## Novel metric describing anoxia in lakes

46 as they are released or processed continuously during anoxia. We believe that anoxic age can be  
47 used to predict the ecological consequences of temporally and spatially growing anoxia.

48

49 Key words: Anoxia, hypolimnion, lakes, anoxic age, oxygen, nutrients, methane, greenhouse gas

50

51 Data availability statement: All raw data and scripts will be available on

52 Github.com/MaxLauLab/AnoxicAge upon manuscript acceptance and attributed a doi using

53 zenodo.org.

54

55

56

## Novel metric describing anoxia in lakes

### 57 Introduction

58 Lakes provide essential ecosystem services (Jane et al. 2021), several of which are threatened by  
59 anthropic activities. Both eutrophication and global warming critically affect dissolved oxygen  
60 (DO) availability in lakes through higher hypolimnetic oxygen demand (Müller et al. 2012) or  
61 reduced hypolimnetic ventilation (Bartosiewicz et al. 2019). These pressures thus threaten more  
62 lake hypolimnia to become or stay anoxic for longer temporal episodes (Jenny et al. 2016;  
63 Matzinger et al. 2010). DO depletion in lake hypolimnia have far-reaching ecological  
64 consequences, including the accumulation of reduced compounds toxic to organisms, loss of  
65 habitats and intensified production of greenhouse gases (Jane et al. 2021, and references therein).  
66 Anoxia is also associated with phosphorus release from redox-sensitive sediment components  
67 (Hupfer and Lewandowski 2008). Monitoring and forecasting of these threats can be improved  
68 through modelling of oxygen dynamics.

69  
70 Modelling approaches commonly differentiate between DO consuming processes in  
71 hypolimnetic sediments and waters (Livingstone and Imboden 1996), where contribution of the  
72 latter may be negligible in oxygen models for deep and clear lakes (Matzinger et al. 2010). These  
73 DO consumption models rely on widely available oxygen data and lake bathymetry and are a  
74 convenient tool to study onset and extent of anoxia, but not its consequences. Approaches to  
75 estimate consequences of anoxia, e.g., phosphorus release, used the lake-scale proportion of  
76 either sediment surface (Nürnberg 1984) or water volume (Foley et al. 2012) affected by anoxia,  
77 but both are insufficient to deconstruct the temporal sequence of anoxia-related processes.  
78 Currently, no modelling approach includes all elements required to fully address lake anoxia,

## Novel metric describing anoxia in lakes

79 including time, benthic and pelagic prokaryotic activity and their associated metabolite dynamics  
80 in the water column.

81  
82 Lake water column chemistry reflects material take-up and release patterns of photosynthetic and  
83 heterotrophic organisms. The aphotic zone is dominated by heterotrophic processing of organic  
84 matter, consuming oxygen and releasing polyphenolic (Dadi et al. 2017) and fluorescent  
85 (FDOM, Burdige et al. 2004) dissolved organic matter (DOM) compounds. Under anoxic  
86 conditions, organic matter is not only the precursor for anaerobic metabolic products ammonium  
87 ( $\text{NH}_4^+$ ) and methane, but also facilitates the production of oxygen-sensitive toxins as  
88 methylmercury and hydrogen sulfide (Acha et al. 2018), all accumulating in the hypolimnion  
89 during summertime anoxia. Thus, the extent and intensity of anoxia determines the quantity of  
90 these substances that will be introduced to surface waters in subsequent turnover events.  
91 However, easily predicting their accumulation remains a challenge.

92  
93 In this study, we explored how to predict the accumulation of a common anaerobic metabolite,  
94  $\text{NH}_4^+$ , soluble reactive phosphorus (SRP) and FDOM solely from lake oxygen data. To this end,  
95 we developed a novel metric, anoxic age, which characterizes how long discrete hypolimnion  
96 layers were DO depleted. Our underlying rationale is that vertical exchange is considered  
97 negligible in stratified hypolimnetic waters (Rippey and McSorley 2009), and major solutes are  
98 either produced in situ or released from the conterminous sediments (Livingstone and Imboden  
99 1996). With anoxic ages, we argue that not only the three compounds used herein, but all other  
100 reduced compounds produced as by-products of anaerobic metabolic pathways may be modelled  
101 with high precision and low effort.

## Novel metric describing anoxia in lakes

102  
103 To establish anoxic age as a widely applicable tool to study anoxia, we calculated anoxic ages  
104 from DO data acquired either in a small number of profiles or from several continuous loggers.  
105 We compared anoxic age values modelled from such widely available data formats to observed  
106 anoxic age values obtained in a specifically instrumented lake, running high-resolution DO  
107 profiler in (bi-)daily casts. We based all calculations on the Livingstone and Imboden (1996)  
108 deductive model between layer-specific oxygen consumption rates ( $J_z$ ) and sediment area to  
109 water volume ratio ( $\alpha(z)$ ). We kept the deductive approach but found that reconstructing daily  
110 hypolimnetic oxygen profiles was improved using non-linear equations, thus allowing for  
111 accurate prediction of anoxic age and hence of anaerobic metabolites, including  $\text{NH}_4^+$ , SRP and a  
112 FDOM component from limited data. Anoxic age thus proves to be an easily modelled metric  
113 describing anoxic lake biogeochemistry that can predict a wide array of compound accumulation  
114 and turnover.

115

## 116 [Materials and methods](#)

### 117 [Study sites](#)

118 We place our research in two eutrophic lakes that develop anoxia during summer stratification:  
119 Lake Arendsee (Germany) and Lake Mendota (USA) (table S1, Kreling et al. 2017; Ladwig et al.  
120 2021). We used (bi-)daily multiparameter profiles (YSI) and 5 oxygen loggers (D-Opto, Zebra-  
121 Tech, New Zealand) data from the Lake Arendsee monitoring program (Hupfer et al. 2019), and  
122 weekly to fortnightly multiparameter profiles (YSI Exo2) from Lake Mendota in 2018 and 2020  
123 (Magnuson et al. 2021).

124

## Novel metric describing anoxia in lakes

### 125 [Anoxic age calculation](#)

126 The anoxic age concept transforms oxygen data below a specified threshold into an information-  
127 bearing and ecologically meaningful variable. In essence, anoxic age reflects the time that passed  
128 since a parcel of water crossed the threshold (Fig. S1). Here, we used a conventional DO  
129 threshold for anoxia, 2 mg O<sub>2</sub> L<sup>-1</sup> (Jenny et al. 2016; Rabalais et al. 2010). Hypolimnetic waters  
130 have decreasing oxygen concentrations that are typically monitored in multiple depths, where  
131 each stratum may be considered as discrete because of negligible turbulent vertical diffusion  
132 (Rippey and McSorley 2009). The anoxic age increases for every consecutive timestep (Day<sub>*i*</sub>) a  
133 water stratum DO concentration (DO<sub>*z*</sub>) is below the chosen threshold (DO<sub>threshold</sub>) (eq. 1), where *i*  
134 and *n* are the first and last day of seasonal stratification, respectively.

$$135 \quad \text{Anoxic age}_z(d) = \begin{cases} \text{DO}_z \leq \text{DO}_{\text{threshold}}, \sum_{i=1}^n \text{Day}_i & (\text{eq. 1}) \\ \text{DO}_z > \text{DO}_{\text{threshold}}, 0 \end{cases}$$

136 Anoxic age calculation requires DO concentration in high spatiotemporal resolution (e.g., daily  
137 and 1 m steps). Since measurements in this resolution are rarely available, oxygen values may be  
138 interpolated from two profiles, or alternatively derived from J<sub>*z*</sub>, themselves calculated from a  
139 small number of oxygen profiles (Livingstone and Imboden 1996). To assess if anoxic age may  
140 be accurately predicted from all common measurement practices, we subsampled observations  
141 from the full datasets of Lake Arendsee (see below).

142

143

144

## Novel metric describing anoxia in lakes

### 145 Morphometry

146 To calculate  $\alpha(z)$ , we used equations 2 and 3, where  $A(z)$  is the lake area at depth  $z$ ,  $A_0$  is the  
147 lake surface area,  $z_m$  is the maximum depth of the lake and  $q$  is a fitting parameter (Livingstone  
148 and Imboden 1996).

$$149 \quad A(z) = A_0(1 - z/z_m)^q \text{ (eq. 2)}$$

$$150 \quad \alpha(z) = q/(z_m - z) \text{ (eq. 3)}$$

151 For both lakes,  $q$  was calculated using the hypsography. Lake Mendota hypsography is available  
152 on <http://www.bathybase.org/Data/100-199/100/> (accessed 2021-10-18) and for Lake Arendsee,  
153 it was calculated following equation 5 in Håkanson (2005). Exponent  $q$  was then used to  
154 calculate  $\alpha(z)$  (eq. 3).

155

### 156 Modelling oxygen

157 Lakes are conveniently monitored in either several campaigns during the stratification season, or  
158 with a small number of depths-discrete loggers, enabling  $J_z$  calculation. Hence, we calculated  $J_z$   
159 in two different ways. We compared  $J_z$  (slopes) of a linear regression of manually selected dates  
160 with a segmented regression using two breakpoints (Muggeo 2008) between DO concentration  
161 and time. Both methods yielded similar values (Fig. S2). We also calculated  $J_z$  for all profile  
162 casts taken 28 days apart when the lake was still in fully oxic condition as a “two oxic profiles”  
163 scenario, and for all three hypolimnetic DO loggers combinations from lake Arendsee.  $J_z$  for  
164 Lake Arendsee are reported in table S2 to S4 and in table S5 for Lake Mendota. We then  
165 compared three different types of equations to best describe the relationship between  $J_z$  and  $\alpha(z)$ .  
166 We used a linear fit, and to capture the asymptotic behavior, used log-linear and exponential-  
167 plateau fits (eq. 4), where  $b$  (non-negative) and  $k$  ( $0 \leq k \leq 15$ ) are fitting parameters, and  $J_{z,\max}$  is  
168 the maximum  $J_z$  fitted as a random parameter by the nlsLM function (Elzhov et al. 2016). The



## Novel metric describing anoxia in lakes

169 best model was chosen using  $R^2$ , lowest root-mean-square error (RMSE) and Akaike Information  
170 Criterion.

171 
$$J_z = J_{z,max} - (J_{z,max} - b) * e^{-k \times \alpha(z)} \text{ (eq. 4)}$$

172 Using these equations, we modelled DO profiles series by assuming that the entire water column  
173 was fully oxygenated at the onset of summer stratification. Because stratification onset date is  
174 unknown, we needed to calibrate dates. To do so, we assigned dates to the DO profile series by  
175 matching a measured profile using lowest RMSE. For Lake Arendsee, we had measurements in  
176 sufficient temporal resolution to also calculate anoxic age directly from observations ( $AnoxA_{obs}$ ),  
177 but only used modelled anoxic ages ( $AnoxA_{mod}$ ) for Lake Mendota. We calculated the anoxic  
178 ages (eq. 1) and compared the first date (as day of year, DOY) on which each stratum became  
179 anoxic with observed first day of anoxia to assess quality of  $AnoxA_{mod}$ .

180

### 181 [Chemical data](#)

182 Concentrations of SRP and  $NH_4^+$  were determined photometrically by molybdenum blue  
183 (Murphy and Riley 1962) and indophenol (Bolleter et al. 1961) methods, respectively, using  
184 segmented flow analysis (Scan++, Skalar Analytical, Netherlands). SRP and  $NH_4^+$  values taken  
185 at non-integer depths were rounded at the nearest integer, and those at 0.5 m increment were  
186 floored as anoxia develops toward the surface. Exo2 FDOM was measured at excitation  
187 wavelength 365 nm, emission wavelength 480 nm and is expressed in quinine sulfate units  
188 (QSU). This peak, here referred to as  $F_{365/480}$  ( $F_{ex/em}$ ), is usually interpreted to indicate  
189 terrestrially derived recalcitrant compounds (peak C, Coble 1996).

190

## Novel metric describing anoxia in lakes

191 All reported  $R^2$  were statistically significant at  $p$ -value  $< 0.01$ . All statistics and modelling were  
192 performed using R version 3.6.2 (R Core Team 2017) and all scripts and data will be available  
193 on [github.com/MaxLauLab/AnoxicAge](https://github.com/MaxLauLab/AnoxicAge) and attributed a doi using Zenodo.

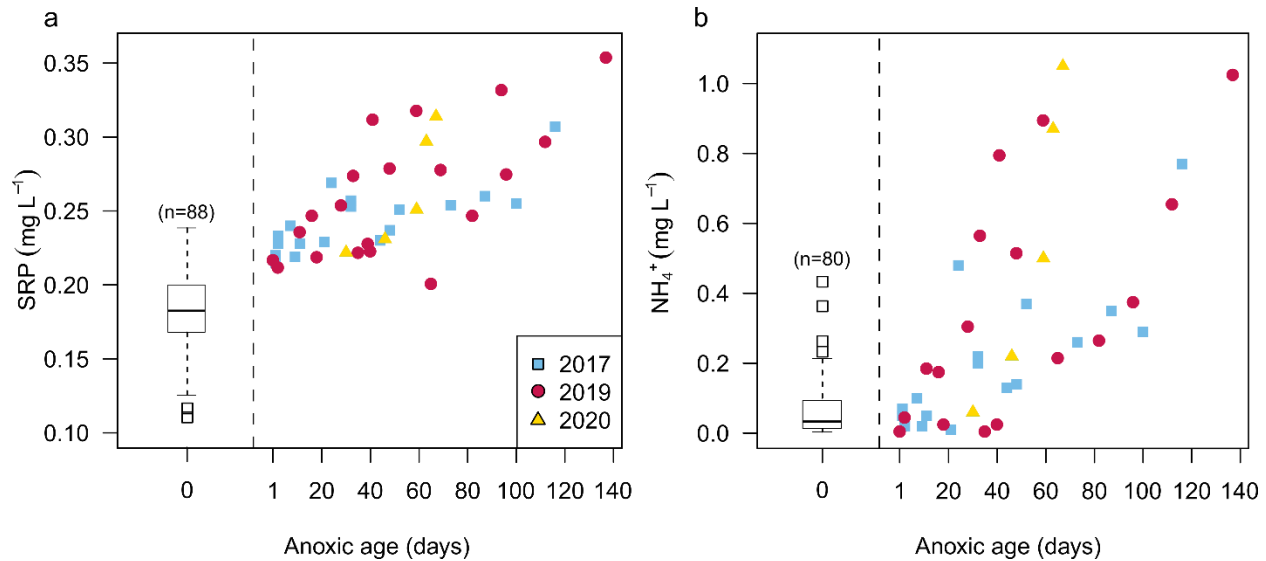
194

## 195 Results

### 196 Nutrients and FDOM

197 We analyzed patterns in SRP and  $\text{NH}_4^+$  from hypolimnetic waters in relation to anoxic age  
198 (AnoxA). When considering anoxic waters ( $\text{AnoxA} > 0$ ) only, we found a good relationship with  
199 SRP ( $R^2 = 0.48$ ), and with  $\text{NH}_4^+$  ( $R^2 = 0.44$ ), where the slopes of these relationships (mean  $\pm$   
200 standard error),  $0.73 \pm 0.11 \mu\text{g SRP L}^{-1} \text{d}^{-1}$  and  $6.0 \pm 1.0 \mu\text{g NH}_4^+ \text{L}^{-1} \text{d}^{-1}$ , represent whole  
201 anaerobic hypolimnion metabolism. Including AnoxA values of 0 (oxic waters) improved the  
202 relationship for both SRP ( $R^2 = 0.62$ ) and  $\text{NH}_4^+$  ( $R^2 = 0.55$ ) but the rates then no longer represent  
203 anaerobic ecosystem-scale metabolism. In both cases, the relationships with DOY or depth alone  
204 were considerably weaker, and when combined explained nearly as much variation as AnoxA  
205 alone, suggesting that AnoxA captures all predictive power of these variables, but adding an  
206 ecologically meaningful interpretation. In multiple regressions, adding depth or DOY to AnoxA  
207 only slightly increased  $R^2_{\text{adj}}$ .

## Novel metric describing anoxia in lakes



208

209 Figure 1. Soluble reactive phosphorus (SRP, a) and ammonium (NH<sub>4</sub><sup>+</sup>, b) as a function of anoxic age in  
210 lake Arendsee. All SRP and NH<sub>4</sub><sup>+</sup> values at an anoxic age of 0 are displayed as a boxplot, with sample  
211 number above. Colored symbols represent different years; blue square: 2017, red circle: 2019 and yellow  
212 triangle: 2020.

213

214 We explored the effect of anoxia on the fluorescent component F<sub>365/480</sub> in lake Mendota using

215 AnoxA<sub>mod</sub>. We found that AnoxA<sub>mod</sub> explained a considerable fraction of F<sub>365/480</sub> variation (Fig.

216 2b and d) with R<sup>2</sup> of 0.63 in 2018 and R<sup>2</sup> of 0.71 in 2020, when all data were considered. When

217 only anoxic values were considered, R<sup>2</sup> were lower at R<sup>2</sup> = 0.56 and 0.58, respectively. Anoxia

218 seemed to have a reproducible, stabilizing influence on this fluorescent component for 30 to 40

219 days (Fig. 2b and d); a behavior not well reflected by linear models and only visualized using

220 AnoxA. In contrast to nutrients, the relationships with time (Fig. 2a and c) were better, with R<sup>2</sup>

221 of 0.84 in 2018 and 0.78 in 2020, respectively. Although time seemed to be a good predictor, its

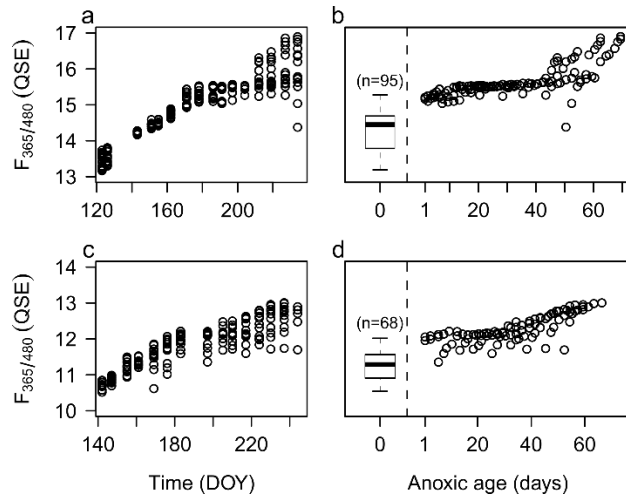
222 predictive power was greatly reduced when only values from anoxic waters were analyzed with

223 R<sup>2</sup> dropping to values of 0.32 to 0.27, respectively, indicating that the change in DOM

224 composition is not constant over time spent in anoxia.

225

## Novel metric describing anoxia in lakes



226

227 Figure 2. Fluorescent component  $F_{365/480}$  as a function of time (a, c) and modelled anoxic age (b, d), for  
228 2018 (top row) and 2020 (bottom row) in lake Mendota.

229

### 230 Modelling anoxic age

231 As AnoxA is calculated from daily DO profiles, we first assessed which type of equation best

232 fitted  $J_z$  to  $\alpha(z)$  from modelled profile time series. This step is critical to interpolate between

233 irregular profile measurements or between missing depths of discrete loggers. The best fit was

234 generally the exponential-plateau (Figures 3 and S3, table S6). When excluding several deep

235 layers by subsampling  $J_z$  to simulate partial anoxia, we found that the exponential-plateau model

236 was slightly less resilient than the log-linear relationship (Fig. S4). Overall, the linear fit was

237 inferior to the other equations in both studied lakes (Fig. 3). The five loggers had lower fits

238 regardless of equations, presumably because of a smaller number of  $\alpha(z)$  values. Subsampling

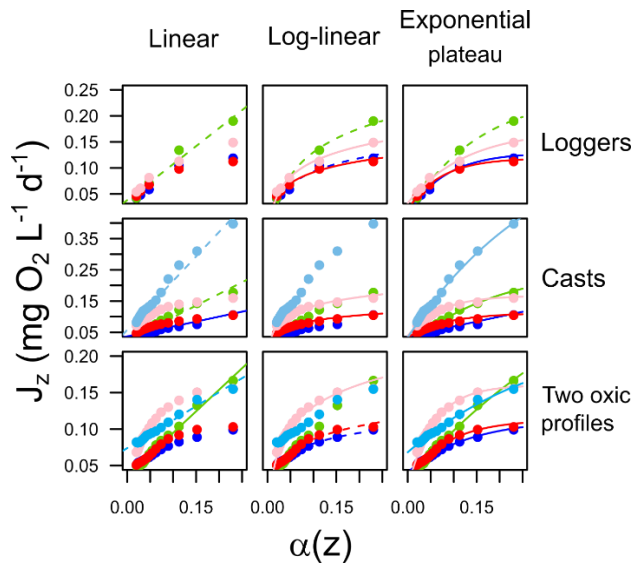
239 three loggers or using only two oxic profiles provided reliable  $J_z$ - $\alpha(z)$  relationships in most cases

240 (Fig. 4).

241

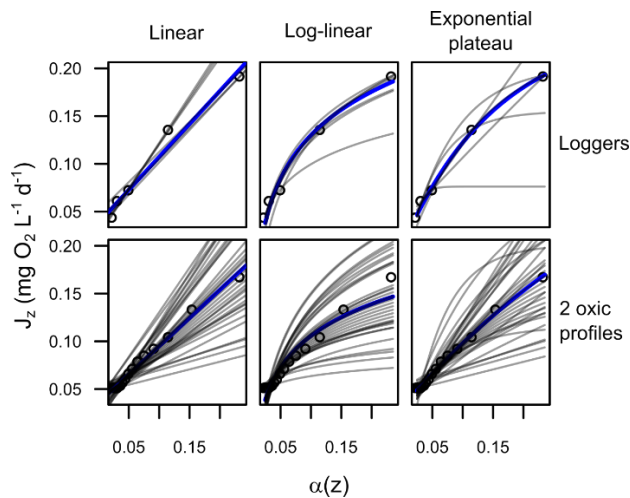
242

## Novel metric describing anoxia in lakes



243

244 Figure 3. Oxygen consumption rates ( $J_z$ ) as a function of sediment area to volume ratio ( $\alpha(z)$ ) in Lake  
 245 Arendsee. The rows represent autonomous loggers, autonomous (daily) YSI casts and the average of the  
 246 two oxyc profiles scenario, respectively. The columns represent the different fitting equations with linear,  
 247 log-linear and exponential-plateau, respectively. Full lines in the different panels indicate fits between  $J_z$   
 248 and  $\alpha(z)$  with  $R^2 > 0.99$ , dashed lines,  $R^2 > 0.97$ . Colors represent different years and are the same for all  
 249 panels: blue (2017); green (2018); red (2019); pink (2020); light blue (2021).  
 250



251

252 Figure 4. Oxygen consumption rates ( $J_z$ ) as a function of sediment area to volume ratio ( $\alpha(z)$ ) in Lake  
 253 Arendsee by subsampling loggers (three, top row) and profiles casts (two, bottom row) to emulate  
 254 common sampling scenarios (grey lines). The blue line represents the relationship using five loggers (top)  
 255 and all profile casts (bottom).  
 256

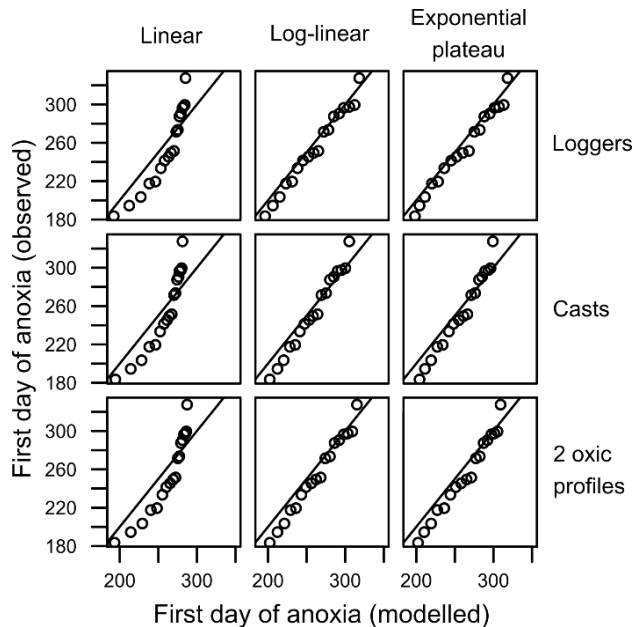
257 Using linear, log-linear and exponential-plateau fits, we then compared their estimations of the

258 date of anoxia's first appearance. For all years and most data source-model type pairs, the log-

## Novel metric describing anoxia in lakes

259 linear and exponential-plateau models yielded good results, whereas the linear relationship did  
260 not (year 2019 in Fig. 5, other years in figures S5 to S8).

261



262  
263 Figure 5. Relationship between observed and modelled first day of strata-specific anoxia in Arendsee,  
264 2019. Each panel is a combination of data source (rows; loggers, autonomous YSI casts and two profiles  
265 during oxic conditions) and  $J_z$  model type (columns; linear, log-linear and exponential-plateau). Each  
266 point is a different hypolimnion depth (1 m increment), and the solid line represents a 1:1 relationship.  
267

## 268 Discussion

269 Water column and sediments heterotrophic respiration and oxidation of reduced compounds  
270 drive oxygen loss in lake hypolimnia (Matzinger et al. 2010; Steinsberger et al. 2020). To study  
271 and predict the specific lake water biogeochemistry that begins with deoxygenation, we  
272 developed a novel, ecologically meaningful metric, anoxic age. To this end, we built on the  
273 deductive approach to deconstruct oxygen depletion rates using lake bathymetry. In the original  
274 approach, fitting parameters of linear regressions directly represent sediments and water DO  
275 consumption rates (Livingstone and Imboden 1996; Rhodes et al. 2017). However, in both lakes  
276 studied herein, non-linear equations with a decreasing slope at higher  $\alpha(z)$  values much better

## Novel metric describing anoxia in lakes

277 approximated the  $J_z$ - $\alpha(z)$  relationships. These observations are consistent with other systems and  
278 can partly be explained by the smaller diffusive DO flux at smaller partial pressure gradients that  
279 dominate the deeper strata (Ladwig et al. 2021; Rippey and McSorley 2009). Non-linear fits  
280 lump areal and volumetric oxygen consumption rates but can predict more accurate daily oxygen  
281 profiles and consequently, anoxic age.

282

## 283 [Nutrients and FDOM](#)

284 We examined the succession of anaerobic processes in lake hypolimnia over time and derived  
285 metabolic rates using linear models of substrate concentration over anoxic age. We estimated a  
286 lake's anoxic ages based on a one-dimensional conceptualization of the water column, assuming  
287 that horizontal diffusivity greatly exceeds vertical diffusivity (Quay et al. 1980). Larger vertical  
288 diffusivity such as during seiching and horizontal turbulence promote vertical exchange among  
289 water layers, decreasing between-layer concentration differences (Rippey and McSorley 2009).  
290 Hence, the observed metabolic rates calculated herein would be slightly underestimated and  
291 therefore represent conservative estimates across all hypolimnetic layers.

292

293 Anoxic age is in essence a space-for-time transformation and examines the accumulation of  
294 anaerobic metabolic byproducts independent from the position in the water column. Therefore,  
295 we expect a stronger coupling of anoxic age with pelagic-driven anaerobic metabolites than with  
296 those related to sediment processes. The fluorescent component  $F_{365/480}$  that increased during  
297 Lake Mendota hypolimnetic anoxia is a dominant fluorescence signature in anoxic marine waters  
298 (Loginova et al. 2016) which suggests the production of recalcitrant DOC from both pelagic  
299 processing and sediment release (Dadi et al. 2017; Lau and del Giorgio 2020). Anoxic age  
300 revealed two stages of anoxic  $F_{365/480}$  transformation: a month-long stabilization followed by a

## Novel metric describing anoxia in lakes

301 strong increase of this component. This behavior remains unexplained by current  
302 conceptualization and would be missed without the anoxic age metric, offering a new lens to  
303 investigate carbon dynamics.

304  
305 We also found good, positive relationships with SRP and  $\text{NH}_4^+$ , two compounds mostly related  
306 to sediment processes (Carey et al. 2022). The SRP increase likely reflected the initial phase of  
307 organic phosphorus diagenetic release, unobstructed by SRP-capturing iron oxides at the  
308 sediment surface (Hupfer and Lewandowski 2008). Classically, this process should be more  
309 pronounced in water layers with a higher  $\alpha(z)$ , yet we found a linear increase with depth-  
310 independent AnoxA, and models including depth as a variable were only slightly better.

311 Similarly, anaerobic  $\text{NH}_4^+$  production is dominated by sediment diagenesis, but also a product of  
312 pelagic microbial dissolved organic nitrogen turnover (Berman et al. 1999), and was adequately  
313 modeled with AnoxA alone. Limitations of molecular diffusion may be responsible for the  
314 depth-independent behavior of anoxic metabolites similar to oxygen consumption in sediments  
315 (Rippey and McSorley 2009). Therefore, a space-for-time analysis can capture the lake-scale  
316 trend of substrate behavior under anoxic conditions.

317

### 318 Modelling oxygen profiles

319 We presented various equations to calculate anoxic age from widely available oxygen  
320 monitoring data. The exponential-plateau provided the best fit between  $J_z$  and  $\alpha(z)$  for most lakes  
321 and years, and the best prediction of first day of anoxia. This test assumed a monotonic DO  
322 decrease, although physical mixing may oxygenate upper hypolimnetic strata even during  
323 stratification (Burns 1995), resulting in a reset of anoxic age to zero. This reset of anoxic age  
324 would be reflected in lake water biogeochemistry as reduced compounds are highly DO sensitive



## Novel metric describing anoxia in lakes

325 and rapidly oxidize (Kappler et al. 2004). This simplification seemed adequate for deep lakes'  
326 hypolimnia but may need critical evaluation in shallower and more wind-exposed lakes. We note  
327 that an unconstrained exponential-plateau equation is particularly sensitive to  $J_z$  at large  $\alpha(z)$ .  
328 However, constraining the equation with *a priori* knowledge of the system provided adequate  
329 extrapolations, similar to the more robust log-linear equation. Thus, we recommend using the  
330 most plausible fit as the objective is to accurately predict anoxic ages.

331  
332 The high temporal and spatial oxygen sampling resolution in Lake Arendsee enabled us to  
333 directly calculate anoxic ages, but also to test result quality of different sampling scenarios. By  
334 subsampling 3 DO loggers and by simulating two profiles per year, we assessed that these low  
335 vertical and temporal sampling resolutions were enough to adequately model oxygen  
336 consumption rates. With only two oxygen profiles, it is possible that deeper parts of the lake are  
337 already anoxic, prohibiting the use of these readings for  $J_z$  calculations. In this scenario, the  
338 linear and exponential-plateau were inadequate, but the log-linear equation nonetheless provided  
339 good  $J_z$ - $\alpha(z)$  approximations. Common lake sampling practices therefore allow daily oxygen  
340 profiles modelling and thus anoxic age calculation.

341  
342 [Future perspectives](#)  
343 Anoxia is pervasive and of growing concern in aquatic ecosystems worldwide (Rabalais et al.  
344 2010), promoted by various anthropic activities including eutrophication and browning (Brothers  
345 et al. 2014; Jenny et al. 2016). We argue that anoxic age can be used across aquatic ecosystems  
346 to predict critical consequences of anoxia. Anoxic age can be tuned to specific  $DO_{\text{threshold}}$  of  
347 interest (table S7) to analyze the effects of anoxia on organisms (Elshout et al. 2013), greenhouse  
348 gases (Bastviken et al. 2002; Richardson et al. 2009) and toxic substances (Achá et al. 2018;

## Novel metric describing anoxia in lakes

349 Jorgensen et al. 1979; Sánchez-España et al. 2017). As lake-specific production rates can be  
350 modelled using anoxic age from limited observations, these production rates will provide  
351 valuable information to study drivers and trends of anaerobic metabolism and aid in assessing  
352 aquatic ecosystems health under global change.

353

## 354 Acknowledgements

355 We would like to thank Sylvia Jordan (IGB) for managing the long-term program in Lake  
356 Arendsee and for her help with data validation. We are grateful to Christiane Herzog and  
357 Thomas Rossoll (IGB) for laboratory work and other technical support. We acknowledge Tobias  
358 Goldhammer (IGB) for discussions and for the support as head of the Chemical Laboratory.  
359 We'd like to thank Tom Shatwell (Helmholtz-Zentrum für Umweltforschung) for insightful  
360 discussions. The monitoring program is partly supported by the State Agency for Flood  
361 Protection and Water Management Saxony-Anhalt (LHW).

362

363

## 364 References

- 365 Achá, D. and others 2018. Algal Bloom Exacerbates Hydrogen Sulfide and Methylmercury  
366 Contamination in the Emblematic High-Altitude Lake Titicaca. *Geosciences* **8**: 438.
- 367 Bartosiewicz, M., A. Przytulska, J. F. Lapierre, I. Laurion, M. F. Lehmann, and R. Maranger.  
368 2019. Hot tops, cold bottoms: Synergistic climate warming and shielding effects increase  
369 carbon burial in lakes. *Limnology and Oceanography Letters* **4**: 132-144.
- 370 Bastviken, D., J. Ejlertsson, and L. Tranvik. 2002. Measurement of Methane Oxidation in Lakes:  
371 A Comparison of Methods. *Environmental Science & Technology* **36**: 3354-3361.
- 372 Berman, T., C. Béchemin, and S. Maestrini, Y. 1999. Release of ammonium and urea from  
373 dissolved organic nitrogen in aquatic ecosystems. *Aquat. Microb. Ecol.* **16**: 295-302.
- 374 Bolleter, W. T., C. J. Bushman, and P. W. Tidwell. 1961. Spectrophotometric Determination of  
375 Ammonia as Indophenol. *Analytical Chemistry* **33**: 592-594.
- 376 Brothers, S. and others 2014. A feedback loop links brownification and anoxia in a temperate,  
377 shallow lake. *Limnol. Oceanogr.* **59**: 1388-1398.

## Novel metric describing anoxia in lakes

- 378 Burdige, D. J., S. W. Kline, and W. Chen. 2004. Fluorescent dissolved organic matter in marine  
379 sediment pore waters. *Mar. Chem.* **89**: 289-311.
- 380 Burns, N. M. 1995. Using hypolimnetic dissolved oxygen depletion rates for monitoring lakes.  
381 *New Zealand journal of marine and freshwater research* **29**: 1-11.
- 382 Carey, C. C. and others 2022. Anoxia decreases the magnitude of the carbon, nitrogen, and  
383 phosphorus sink in freshwaters. *Global Change Biology* **28**: 4861-4881.
- 384 Coble, P. G. 1996. Characterization of marine and terrestrial DOM in seawater using excitation-  
385 emission matrix spectroscopy. *Mar. Chem.* **51**: 325-346.
- 386 Dadi, T., M. Harir, N. Hertkorn, M. Koschorreck, P. Schmitt-Kopplin, and P. Herzsprung. 2017.  
387 Redox Conditions Affect Dissolved Organic Carbon Quality in Stratified Freshwaters.  
388 *Environmental Science & Technology* **51**: 13705-13713.
- 389 Elshout, P. M. F., L. M. Dionisio Pires, R. S. E. W. Leuven, S. E. Wendelaar Bonga, and A. J.  
390 Hendriks. 2013. Low oxygen tolerance of different life stages of temperate freshwater  
391 fish species. *Journal of Fish Biology* **83**: 190-206.
- 392 Elzhov, T. V., K. M. Mullen, A.-N. Spiess, and B. Bolker. 2016. minpack.lm: R interface to the  
393 Levenberg-Marquardt nonlinear least-squares algorithm found in MINPACK, plus  
394 support for bounds. R package 1.2-1.
- 395 Foley, B., I. D. Jones, S. C. Maberly, and B. Rippey. 2012. Long-term changes in oxygen  
396 depletion in a small temperate lake: effects of climate change and eutrophication.  
397 *Freshwater Biology* **57**: 278-289.
- 398 Håkanson, L. 2005. The Importance of Lake Morphometry for the Structure and Function of  
399 Lakes. *International Review of Hydrobiology* **90**: 433-461.
- 400 Hupfer, M., A. Kleeberg, and J. Lewandowski. 2019. Internal pools and fluxes of phosphorus in  
401 dimictic lake Arendsee, Northeastern Germany, p. 169-185. *In* A. D. Steinman and B.  
402 Spears [eds.], *Internal phosphorus loading in lakes : causes, case studies, and*  
403 *management*. J. Ross Publishing.
- 404 Hupfer, M., and J. Lewandowski. 2008. Oxygen Controls the Phosphorus Release from Lake  
405 Sediments – a Long-Lasting Paradigm in Limnology. *International Review of*  
406 *Hydrobiology* **93**: 415-432.
- 407 Jane, S. F. and others 2021. Widespread deoxygenation of temperate lakes. *Nature* **594**: 66-70.
- 408 Jenny, J.-P. and others 2016. Urban point sources of nutrients were the leading cause for the  
409 historical spread of hypoxia across European lakes. *Proceedings of the National Academy*  
410 *of Sciences* **113**: 12655.
- 411 Jorgensen, B. B., J. G. Kuenen, and Y. Cohen. 1979. Microbial transformations of sulfur  
412 compounds in a stratified lake (Solar Lake, Sinai)1. *Limnol. Oceanogr.* **24**: 799-822.
- 413 Kappler, A., M. Benz, B. Schink, and A. Brune. 2004. Electron shuttling via humic acids in  
414 microbial iron(III) reduction in a freshwater sediment. *FEMS Microbiology Ecology* **47**:  
415 85-92.
- 416 Kreling, J., J. Bravidor, C. Engelhardt, M. Hupfer, M. Koschorreck, and A. Lorke. 2017. The  
417 importance of physical transport and oxygen consumption for the development of a  
418 metalimnetic oxygen minimum in a lake. *Limnol. Oceanogr.* **62**: 348-363.
- 419 Ladwig, R. and others 2021. Lake thermal structure drives interannual variability in summer  
420 anoxia dynamics in a eutrophic lake over 37 years. *Hydrology and Earth System Sciences*  
421 **25**: 1009-1032.
- 422 Lau, M. P., and P. del Giorgio. 2020. Reactivity, fate and functional roles of dissolved organic  
423 matter in anoxic inland waters. *Biology Letters* **16**: 20190694.

## Novel metric describing anoxia in lakes

- 424 Livingstone, D. M., and D. M. Imboden. 1996. The prediction of hypolimnetic oxygen profiles: a  
425 plea for a deductive approach. *Can. J. Fish. Aquat. Sci.* **53**: 924-932.
- 426 Loginova, A. N., S. Thomsen, and A. Engel. 2016. Chromophoric and fluorescent dissolved  
427 organic matter in and above the oxygen minimum zone off Peru. *Journal of Geophysical*  
428 *Research: Oceans* **121**: 7973-7990.
- 429 Magnuson, J. J., S. R. Carpenter, and E. H. Stanley. 2021. Lake Mendota Multiparameter Sonde  
430 Profiles: 2017 - current ver 2. Environmental Data Initiative.
- 431 Matzinger, A., B. Müller, P. Niederhauser, M. Schmid, and A. Wüest. 2010. Hypolimnetic  
432 oxygen consumption by sediment-based reduced substances in former eutrophic lakes.  
433 *Limnol. Oceanogr.* **55**: 2073-2084.
- 434 Muggeo, V. 2008. Segmented: An R Package to Fit Regression Models With Broken-Line  
435 Relationships.
- 436 Müller, B., L. D. Bryant, A. Matzinger, and A. Wüest. 2012. Hypolimnetic Oxygen Depletion in  
437 Eutrophic Lakes. *Environmental Science & Technology* **46**: 9964-9971.
- 438 Murphy, J., and J. P. Riley. 1962. A modified single solution method for the determination of  
439 phosphate in natural waters. *Analytica Chimica Acta* **27**: 31-36.
- 440 Nürnberg, G. K. 1984. The prediction of internal phosphorus load in lakes with anoxic  
441 hypolimnial. *Limnol. Oceanogr.* **29**: 111-124.
- 442 Quay, P. D., W. S. Broecker, R. H. Hesslein, and D. W. Schindler. 1980. Vertical diffusion rates  
443 determined by tritium tracer experiments in the thermocline and hypolimnion of two  
444 lakes1,2. *Limnol. Oceanogr.* **25**: 201-218.
- 445 R Core Team. 2017. R: A language and environment for statistical computing. Vienna, Austria:  
446 R Foundation for Statistical Computing. URL <https://www.R-project.org/>.
- 447 Rabalais, N. N., R. J. Díaz, L. A. Levin, R. E. Turner, D. Gilbert, and J. Zhang. 2010. Dynamics  
448 and distribution of natural and human-caused hypoxia. *Biogeosciences* **7**: 585-619.
- 449 Rhodes, J., H. Hetzenauer, M. A. Frassl, K.-O. Rothhaupt, and K. Rinke. 2017. Long-term  
450 development of hypolimnetic oxygen depletion rates in the large Lake Constance. *Ambio*  
451 **46**: 554-565.
- 452 Richardson, D., H. Felgate, N. Watmough, A. Thomson, and E. Baggs. 2009. Mitigating release  
453 of the potent greenhouse gas N<sub>2</sub>O from the nitrogen cycle – could enzymic regulation  
454 hold the key? *Trends in Biotechnology* **27**: 388-397.
- 455 Rippey, B., and C. McSorley. 2009. Oxygen depletion in lake hypolimnia. *Limnol. Oceanogr.*  
456 **54**: 905-916.
- 457 Sánchez-España, J. and others 2017. Anthropogenic and climatic factors enhancing hypolimnetic  
458 anoxia in a temperate mountain lake. *Journal of Hydrology* **555**: 832-850.
- 459 Steinsberger, T., R. Schwefel, A. Wüest, and B. Müller. 2020. Hypolimnetic oxygen depletion  
460 rates in deep lakes: Effects of trophic state and organic matter accumulation. *Limnol.*  
461 *Oceanogr.*

462